Identifying Descriptors for Solvent Stability in Nonaqueous Li–O$_2$ Batteries

Abhishek Khetan,[†] Heinz Pitsch,[†] and Venkatasubramanian Viswanathan*[,‡]

[†]Institute for Combustion Technology, RWTH, Aachen, Germany, 52056

[‡]Department of Mechanical Engineering, Carnegie Mellon University, Pittsburgh, Pennsylvania, 15213, United States

Ⓢ Supporting Information

ABSTRACT: One crucial challenge in developing rechargeable Li–O$_2$ batteries is to identify a stable solvent that is resistant to decomposition in the electrochemical environment of Li$_2$O$_2$. We attempt to identify descriptors that could be used to test for solvent stability. We build on the recent quantitative experimental results on oxygen consumption and release during discharge and charge respectively. We limit our focus to understanding trends in oxidative stability of solvents and based on a systematic treatment of the electrochemical environment of Li$_2$O$_2$, we propose that, to a first approximation, the highest occupied molecular orbital (HOMO) level could be a good descriptor. We demonstrate that this descriptor correlates well with the experimentally measured degree of rechargeability. We utilize this descriptor to screen a large number of solvents and identify several solvents that could enhance the rechargeability of nonaqueous Li–O$_2$ batteries. We provide a comprehensive compilation of available computational and experimental data of several key solvent parameters that we believe will be the genesis for an 'electrolyte genome'.

SECTION: Energy Conversion and Storage; Energy and Charge Transport
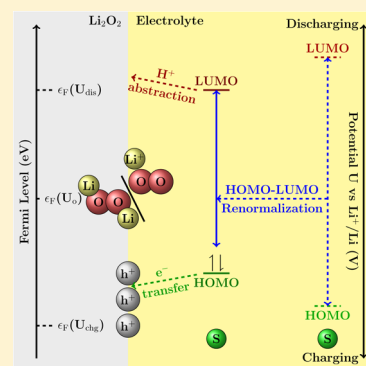
There has been a tremendous interest in nonaqueous Li–air (or Li–O$_2$) batteries owing to its high specific energy.[1,2] However, there are several challenges still remaining in developing practical Li–air batteries.[3] We have previously argued that the two most challenging problems facing Li–O$_2$ batteries are (i) sudden death during deep discharge due to loss in conductivity of the discharge product,[4−6] which ultimately limits the capacity,[7] and (ii) the decomposition of electrolyte and carbon cathode, which imposes severe limitations on the rechargeability of the Li–O$_2$ batteries.[8]

Many galvanostatic studies of nonaqueous Li–O$_2$ cells have focused on electrolyte decomposition, one of the most detrimental processes during a Li–O$_2$ battery operation, even for the relatively stable ether-based solvents.[9] Early experimental investigations by Laoire et al.[10,11] focused on the influence of aprotic solvents and salts on the oxygen reduction reaction (ORR). Using Pearson's Hard Soft Acid Base (HSAB) theory, they proposed that solvents with a higher Gutmann donor number (DN), which indicates their electron donating tendency in their capacity as a Lewis base, lower the Lewis acidity of the Li$^+$ cation, thus stabilizing its complex with the O$_2^-$ anion, a weak Lewis base.

Theoretical calculations for a large number of different classes of solvents using higher order quantum chemical methods in an implicit Poisson−Boltzmann continuum solvation model have been performed by Bryantsev et al. in a series of recent investigations.[12−16] Based on these investigations, it was proposed that solvents with pK_a ≥ 35 were relatively stable against degradation by H abstraction. It was

proposed that a value of ΔG_{act} ≥ 24 kcal/mol could be chosen as a criterion for stability against nucleophilic substitution. Using these criteria in combination with cyclic voltammetry, the authors rationalized why certain classes of solvents like esters, sulfones, phospates, and carbonates were unstable against degradation. Although the explicit formation of Li–O$_2$ discharge products and their interaction with the solvent were not considered, these investigations paved the way for a descriptor-based approach for identifying stable solvents.

Recently, McCloskey et al.[8,17] performed a series of thorough experiments on nonaqueous Li–O$_2$ batteries using in situ quantitative differential electrochemical mass spectrometry (DEMS) and ex-situ analysis of discharge products at the cathode using X-ray diffraction (XRD), NMR and Raman spectroscopy for a number of relevant solvents. In their studies, they have defined and made use of very intuitive and powerful measures of cell performance: number of electrons per O$_2$ transferred during discharge (e$^-$/ORR) and charge (e$^-$/OER (oxygen evolution reaction)) process.[17] Ideally, both the formation and decomposition of Li$_2$O$_2$ should yield 2e$^-$ per O$_2$ molecule. However, this quantity actually deviates from a 2e$^-$/O$_2$ during battery operation, indicating the presence of undesirable parasitic processes. Further, one can assert that the larger the deviation, the less efficient and rechargeable the cell is.
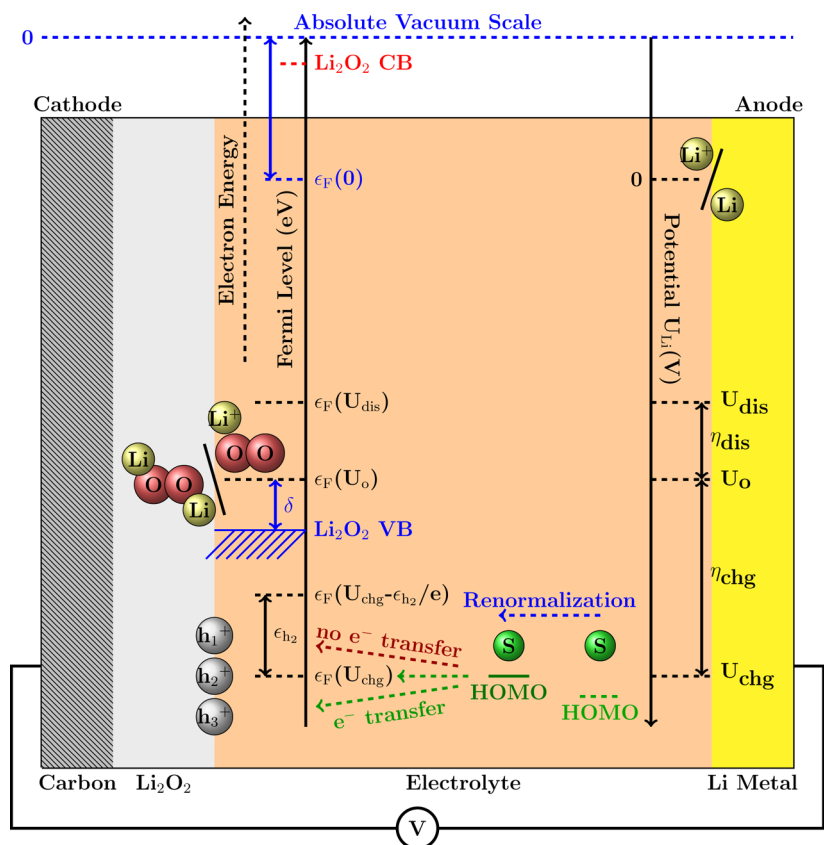
Figure 1. The alignment of the Fermi level, ε_F, at cathode (left) with respect to the electrode potential U_{Li} versus the Li/Li$^+$ redox couple at anode (right) on the AVS (dashed blue line above), the band energy levels of Li$_2$O$_2$ and a schematic representation of HOMO−LUMO gap renormalization before electron transfer. The Li/Li$^+$ redox couple is located at $\varepsilon_F(0) \simeq 1.4$ V versus the AVS. The electrode potential essentially shifts the free energy of electrons at cathode down on Fermi level scale by $\Delta G = -eU$. At equilibrium potential $U_{Li} = U_o$, the Fermi level at the cathode is, $\varepsilon_F(U_o)$. Bulk electrolysis discharge experiments have predicted that the VBM of Li$_2$O$_2$ is pinned at $\delta \simeq 0.4$ eV below the Fermi level at equilibrium (hashed blue line), which now sets the band levels of Li$_2$O$_2$ on the same reference scale. During discharge and charge, the Fermi level of the Li$_2$O$_2$ surface shifts up by $e\eta_{dis}$ and down by $e\eta_{chg}$, respectively. On the other hand, when the solvent molecule, 'S', approaches the cathode surface, there is a renormalization of its HOMO and LUMO levels leading to HOMO−LUMO gap shrinking. An electron transfer from the solvent to the hole states is possible depending on the relative location of the hole state above the Fermi level at the given charging potential U_{chg}. If upon occupation of the hole, the energy level of the electron is lower than its HOMO energy in the solvent, such a transfer is very probable.

During discharge, McCloskey et al.[8] found that for a number of solvents such as dimethoxyethane (DME), dimethyl sulfoxide (DMSO), N-methylpyrrolidinone (NMP), tetrahydrofuran (THF), acetonitrile (MeCN), triglyme (TGE), etc., the e$^-$/ORR mostly remains confined to a 2e$^-$/O$_2$ limit within a nominal error limit ($\leq$5%) with a similar discharge overpotential. One must carefully note, however, that a nearly 2e$^-$/O$_2$ discharge behavior does not guarantee that all the electrons are involved in formation of stoichiometric Li$_2$O$_2$. This was shown in a subsequent study using a novel titration protocol,[17] that even in the most stable system (1N LiTFSI/DME), only 91% of the expected Li$_2$O$_2$ yield was obtained. The loss in Li$_2$O$_2$ yield has been attributed to Li$_2$O$_2$ induced decomposition of the electrolyte solvent and also the electrolyte salt, based on the observation of LiF using NMR measurements. Carbonate formation due to oxidation of the carbon cathode was found to be small compared to the aforementioned degradation mechanisms during discharge. Recent experimental investigations by Luntz et al.,[7] have explicitly shown the independence of the charging over-potentials with respect to the extent of discharge. The potential independence indicates that the degradation process during discharge is not electrochemical in nature. However, the chemical stability of solvent during discharge is indispensable to achieving high Li$_2$O$_2$ yield.[17]

During charge, however, the same set of solvents deviate from an ideal 2e$^-$/O$_2$ process in markedly different ways.[8] On a careful look at the charge curves of each of these solvents, it can be seen that the onset potentials, i.e., the potentials at which the e$^-$/OER increases above the ideal 2e$^-$/O$_2$ process, vary from solvent to solvent. Further, it can be observed that the deviation, which is initially less, increases progressively along with the rise in the cell potential and fall in O$_2$ evolution during charging. The (e$^-$/ORR) and (e$^-$/OER) data have been reproduced in Table S1 as given by McCloskey et al.[8] In a subsequent study, where McCloskey et al.[17] quantified Li$_2$O$_2$ oxidation as well as O$_2$ evolution simultaneously, it was seen that during the charge process, the OER rate is less than the oxidation rate of Li$_2$O$_2$, which implies that a part of Li$_2$O$_2$ is getting oxidized in other parasitic processes. This lends support to the argument presented earlier that the parasitic processes due to Li$_2$O$_2$ induced electrolyte decomposition and carbon cathode oxidation eventually lead to formation of interfacial carbonate layers.[18]

However, there are still numerous gaps in the rapidly evolving picture of solvent degradation. In this Letter, we aim

to fill some of these gaps by identifying properties inherent to the solvent that can act as descriptors of solvent stability and thus rechargeability. On the basis of the discussions above, we adopt e^-/OER as the marker for the stability of solvent against oxidation. The closer this quantity is to an ideal $2e^-$/O_2 process, the less is the loss of electrons to parasitic processes due to solvent oxidation. We show that the chosen metric, e^-/OER, correlates well with the true rechargeability metric, ORR/OER, and this is discussed in the Supporting Information. We connect the effect of the Li–O_2 discharge products and electrode potential in a unified way in an effort to understand the origins of the lowering of the oxidative stability of the solvents. We use this unified treatment to argue that the highest occupied molecular orbital (HOMO) level of the solvent could be a good descriptor for solvent reactivity and demonstrate a good correlation with the experimentally measured degree of rechargeability.

To understand the solvent stability in the electrochemical environment of Li_2O_2, we first develop a unified framework to treat the electrode potential at cathode, U_{Li} vs the Li/Li^+ redox couple, the Fermi level of the discharged Li–O_2 products, ε_F, and the band levels of bulk Li_2O_2. A natural choice for such a reference is the absolute vacuum scale (AVS),[19] which places the standard hydrogen electrode (SHE) at $\simeq 4.44$ V with respect to electrons at rest (0 V). To connect the electrode potential scale to the AVS, we note that the Li/Li^+ redox couple is positioned at $\simeq -3.05$ V vs SHE, which will then set it at $\simeq 1.4$ V on the AVS, as shown in Figure 1. When the cell is operating at any given electrode potential U, the free energy of the electrons at the carbon cathode shifts by an amount, $\Delta G = -eU$. It is to be noted that the electron energy runs in the direction opposite to that of the electrode potential. Therefore, the Fermi level of the electrons at the carbon cathode, ε_C, can now be directly related to any changes in the electrode potential.

To connect the Fermi level of the Li–O_2 discharge products, ε_F, to the AVS, it is of utmost importance to note that equilibrium at the carbon–Li_2O_2 interface demands that the Fermi level of carbon cathode, ε_C, is always aligned with it, i.e., $\varepsilon_F = \varepsilon_C$. This occurs due to the fact that the Debye length of the Li_2O_2 is much larger than the thickness of practically achievable discharge films, and there is no screening of potential within the Li_2O_2 film.[7] Any changes in the electrode potential can thus be directly translated to changes in the Fermi level of the Li–O_2 discharge products. Following the same line of argument, at the cell equilibrium potential of $U_o \simeq 2.96$ V, the corresponding Fermi level at the cathode, $\varepsilon_F(U_o)$, is U_o below U_{Li/Li^+}. During discharge at U_{dis}, the free energy of the electron on the Fermi level scale shifts up relative to $\varepsilon_F(U_o)$ by $e\eta_{dis} = e(U_o - U_{dis})$. In a similar way, during charge, the electron is stabilized by $e\eta_{chg} = e(U_{chg} - U_o)$, as shown in Figure 1.

Having referenced both U_{Li} and ε_F to the AVS, one can now place the band energy levels of Li_2O_2 on the AVS. Li_2O_2 is generally understood to be a wide-band gap insulator. While an experimentally measured value of the Li_2O_2 band gap is not yet available, there have been several computational investigations at different levels of theory and accuracy, which have predicted the difference between its valence band maximum (VBM) and conduction band minimum (CBM) energy levels to be in the range 4.2–6.8 eV.[20–25] Although the precise locations of the VBM and CBM are not known on the AVS, it has been argued on the basis of bulk electrolysis Li–O_2 discharge experiments that the VBM resides at $\delta \simeq 0.4$ eV below the Fermi level at

U_o.[6] As illustrated in Figure 1, the VBM of Li_2O_2 can now be pinned below $\varepsilon_F(U_o)$, thus completing the picture of the relative locations of all the relevant energy levels on the same reference.

The characteristic molecular energy levels for solvents in the bulk are their HOMO and lowest unoccupied molecular orbital (LUMO) levels. We stipulate that the locations of these levels are crucial to solvent stability, both during discharge and charge. For example, during charging at any potential U, there is a population of hole and defect states on the Li_2O_2 surface distributed over a range of energy levels both above and below the corresponding Fermi level $\varepsilon_F(U)$. The presence of such states naturally implies more instances when charge transfer can occur. Although, the solvent HOMO levels can be expected to be significantly deeper that the surface Fermi level, the availability of an electron residing at the HOMO of the solvent molecule makes it susceptible to oxidation via a charge transfer to a hole or defect state of an appropriate energy level. The calculation of all possible surface states is extremely difficult. Nevertheless, one can assert that the lower the HOMO level, the lesser is the tendency to give away electrons to the Li_2O_2 surface states. On this basis, we propose that the tendency of such a transfer is directly correlated with the location of the solvent HOMO level. This hypothesis is in agreement with the fact that solvent degradation is accelerated at higher potentials, which basically implies that the hole and defect states are now distributed around an even lower surface Fermi level.

One must note, however, that a solvent's HOMO–LUMO gap shrinks when the molecules moves closer to the reaction surface, as was explained by Garcia-Lastra et al.[26] Classically, the effect can be understood in a way analogous to the creation of an image charge on a substrate due to its dynamic polarization. This leads to a renormalization of both the HOMO and LUMO levels of the solvent molecule upon physisorption, thus shrinking its electrochemical stability window. Their results indicate a simultaneous raising of HOMO level and lowering of LUMO level of a solvent molecule, and this is more pronounced when the surface is metallic in nature. Even though Li_2O_2 is generally understood to be a wide-band gap insulator, its surface, specially in its nonstoichiometric condition, has been shown to be metallic in nature.[27] Therefore, the effect of renormalization cannot be completely ignored, as has been illustrated in Figure 1. However, to a first approximation, we expect that the quantitative trends in HOMO–LUMO gap renormalization for various solvents over the same surface will be similar.

A good descriptor for performance characteristics such as catalytic activity, or in this case solvent stability, is one that can be computed easily and requires minimal user intervention to calculate. In that sense, the HOMO level for aprotic solvents in Li–O_2 batteries can be considered a good descriptor, because it can be easily computed for a large number of solvents that satisfy other requirements from an application point of view. In Figure 2, we plot our chosen marker of oxidative solvent stability, i.e., e^-/OER borrowed from the work of McCloskey et al.,[8] against the calculated values of HOMO levels for different solvents (DME, THF, DMSO, MeCN). The calculated HOMO values in vacuum for these different solvents were all chosen at the MP2=Full 6-31G* level from the NIST database[28] to ensure consistency. We also show insensitivity to the choice of the level of theory used for calculating HOMO values (see Figures S1, S2, and S3). As can be clearly seen, solvents with lower HOMO levels fare much better in terms of
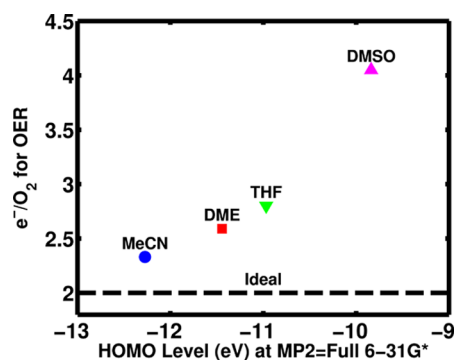
Figure 2. Correlation between solvent HOMO levels (eV) and electrons released during OER (e^-/O_2), taken from the work of McCloskey et al.[8] In an ideal solvent, the e^-/O_2 value is 2, because $Li_2O_2 \rightarrow 2Li^+ + O_2 + 2e^-$ is a 2 e^- process. The HOMO level values were all taken from NIST's CCCBDB database[28] and have been computed at the same level of theory, i.e., MP2=FULL 6-31 G*. The trends observed in this correlation are insensitive to the choice of theory as shown in Figures S1, S2, and S3. The solvents for which both values were available were used: MeCN, DME, THF, and DMSO. The HOMO level values and e^-/OER date are tabulated in Table S1.

electrons generated for O_2 evolution. Therefore, we propose that the HOMO levels of solvents can be used an effective descriptor, to a first approximation, in search for better solvents for Li−O$_2$ systems. We would like to emphasize that we believe that the HOMO level in vacuum is more appropriate for describing stability at the electrochemical solid−liquid interface. This is based on the fact that the solvent is expected to have minimal solvation at the solid−liquid interface.

A brief discussion on the effectiveness of other descriptors such as Gutmann Donor number, acid dissociation constant, pK_a, and the Gibbs activation energy for the nucleophilic substitution reaction, ΔG_{act}, as suggested in the work of Bryantsev et al.[12,13,16] and Laoire et al.[11] has been presented in the Figures S4, S5, and S6 in the Supporting Information. Among these, the Gutmann DN has a firm physical basis[11,29] and shows reasonable correlation with the experimentally measured degree of rechargeability. However, the determination of DNs is beset by variations in the value for a given solvent. The amount of solvation is an inexact quantity, and its measurement and calibration is a function of the experimental technique.[30] Therefore, we argue that the HOMO level is a more appropriate choice for a descriptor-based screening study.

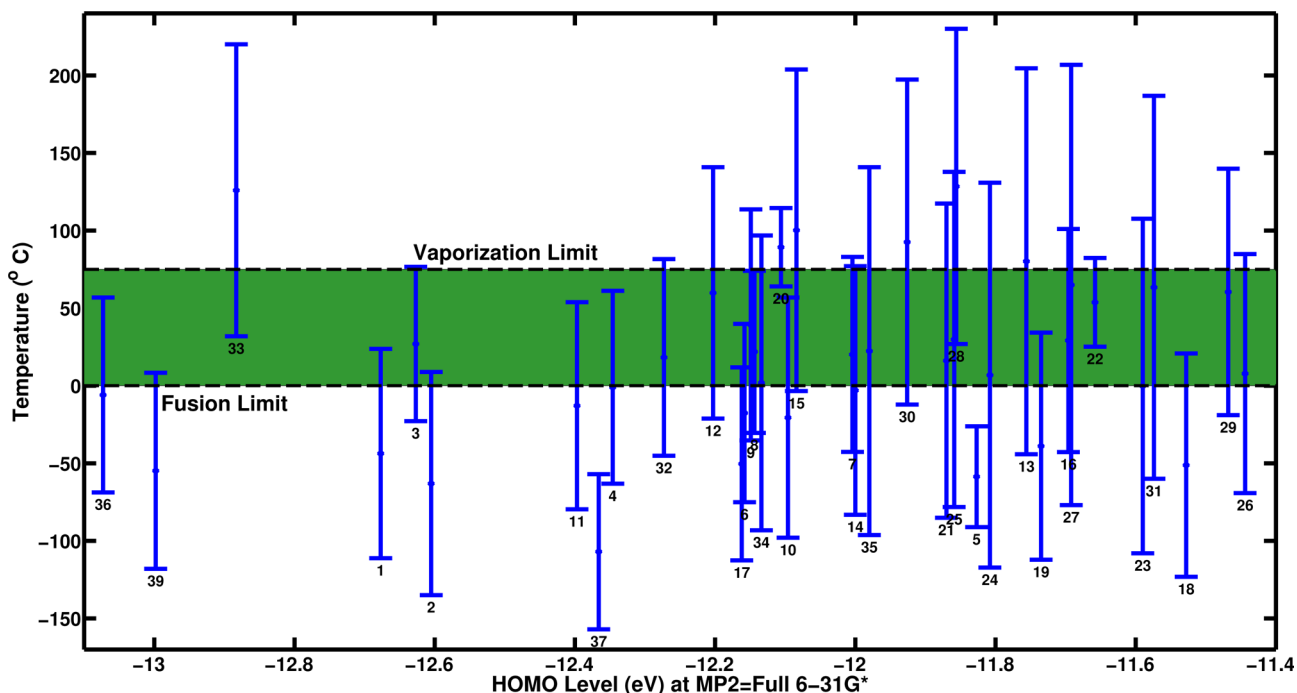To demonstrate the usefulness of the HOMO level as a descriptor, we surveyed hundreds of solvents for relevant

Figure 3. Screening for stable solvents using the HOMO level (eV) as a descriptor and temperature range (°C) of solvents' liquid state. The boiling point is shown as the upper limit of the bar and the melting point is the lower limit. Hence, the length of the line along the temperature axis simply denotes the range over which the solvent is in liquid state. The fusion limit set at 0 °C and the vaporization limit set at 75 °C are guiding lines denoting a minimum desired temperature window for solvents' liquidity. Solvents with absolutely no overlap of their liquid state with this window will probably be inapplicable in practical systems. Phase change data used here have been borrowed from the NIST database.[32,33] Only solvents with HOMO level value ≤ −11.444 eV (DME) have been considered as candidates. The HOMO level values were all taken from NIST's CCCBDB database[28] and have been computed at the same level of theory, i.e., MP2=FULL 6-31 G*. The numbers corresponding to each solvent are the same serial numbers as tabulated in Table S2 as follows: trichlorofluoromethane[1], fluorodichloromethane[2], carbon tetrachloride[3], trichloromethane[4], chloromethane[5], dichloromethane[6], 1,2-dichloroethane[7], 1,1,1-trichloroethane[8], 1,1,2-trichloroethane[9], methyl acetate[10], ethyl formate[11], propanoic acid[12], γ-butyrolactone[13], ethyl acetate[14], hexanoic acid[15], methyl pivalate[16], ethylene oxide[17], acetaldehyde[18], propylene oxide[19], 1,3,5-trioxane[20], 1-butanol[21], 1,1-dimethylethanol[22], 2-methyl-1-propanol[23], 3-methyl-1-butanol[24], 1-pentanol[25], 1,2-dimethoxyethane[26], 1,3-butanediol[27], 1,4-butanediol[28], cyclopentanol[29], ethylene glycol[30], propylene glycol[31], acentonitrile[32], malononitrile[33], propionitrile[34], pentanenitrile[35], tetrachlorosilane[36], methyl silane[37], methyl hypochlorite[38], and carbondichloride[39].

physical properties, as tabulated in Table S2 and S3. Practically applicable solvents must also satisfy criteria such as low melting point (MP), high boiling point (BP), high dielectric constant and conductivity, low viscosity and toxicity, and, in the case of Li−O$_2$ batteries, also high oxygen solubility.[31] Though it is quite difficult to find a single solvent meeting all requirements, the richness of organic chemistry can ensure that such a problem can be overcome with blends of solvents, as has been successfully seen in Li-ion batteries. Keeping these factors in mind, we restrict our discussion to finding HOMO values for acceptable stability with the solvents' liquid state being the only constraint.

As can be seen in Figure 3, we plot the solvents' HOMO level and the liquid phase temperature window for these solvents. Setting DME[26] with a HOMO level value = −11.444 eV as the benchmark for acceptable solvent stability, only those solvents were considered whose HOMO level values were less than this value. It can be seen that there are quite a few solvents that have never been known to be used in Li−O$_2$ systems but may turn out to be quite stable and exist in the liquid state in the temperature range 0−75 °C. Esters (γ-butyrolactone[13], ethyl acetate[14], and methyl pivalate[16]) could possibly be good candidates owing to the presence of a stable (−COO−) group. Likewise, nitrile based solvents (acetonitrile[32], propionitrile[34], and pentanenitrile[35]) are seemingly excellent candidates, probably due to the presence of a highly electronegative (−CN) group. Several acids and alcohols (propanoic acid[12], hexanoic acid[15], 1-butanol[21], 2-methyl-1-propanol[23], 3-methyl-1-butanol[24], 1-pentanol[25], 1,3-butanediol[27], cyclopentanol[29], ethylene glycol[30], and propylene glycol[31]) have comparably good HOMO level values and also a wide liquid state temperature window. However, the presence of the (−OH) group makes them H$^+$ donors. Although such solvents might fare well during charging, they may be at risk of H abstraction during discharge.

Besides these, there are several solvents with acceptable HOMO level values but do not completely satisfy the liquid state criterion. Helpful trends can be seen to emerge from the collected data, which can contribute to our understanding of what could make a good blend of solvents. For instance, chloroflouromethanes (1−9) and silanes ([36], [37]) have favorably low HOMO level values; however, most of them do not exist in liquid phase in the temperature range 0−75 °C. The few that do are highly toxic and entail environmental hazards. The observation that flourination and chlorination lowers the HOMO levels of common organic solvents, however, can be applied for improving solvent stability. This lowering of solvent HOMO level can be explained as a result of the addition of −F and −Cl, which are highly electronegative. Not surprisingly, flourination of β-carbon positions in ethers has been proposed as a way to increase solvent stability in the recent work of Bryantsev et al.[14]

The surveyed solvents were also examined for other properties desired in a liquid electrolyte systems as mentioned before. However, owing to a dearth of data on physical and chemical properties, we have chosen to tabulate them in Table S3 with a view to compile a comprehensive database. We believe this will serve as the genesis of an 'electrolyte genome' which can help accelerate solvent discovery for batteries.

While this work is an important first stride in the direction of understanding the solvent stability during charging in Li−O$_2$ battery systems, there are several other criteria that need to be satisfied. Stability against oxidation is only one side of the entire picture of solvent stability. The propensity of solvents to withstand hydrogen abstraction during discharge needs to be investigated thoroughly to eventually realize a Li−O$_2$ battery. Investigations on the same are underway, although there is a dearth of experimental data on the chemical stability of solvents during discharge. Further, the effect of added salts in the electrolyte could play a crucial role in affecting solvent stability. This presents an exciting new frontier, and we hope that our theoretical investigations will encourage experimentalists to test some of the new candidates identified in this work.

■ ASSOCIATED CONTENT

ⓢ Supporting Information
Figures S1, S2 and S3 show the insensitivity to the choice of level of theory for HOMO level values. Table S1 tabulates the experimentally measured e$^-$/O$_2$ during ORR and OER, HOMO level, and Gutmann DN for various solvents. Table S2 is a compendium of solvents that passed the chosen stability criterion. Table S3 is a comprehensive list of all other solvents that were also considered for this study. Figure S4 shows the correlation between e$^-$/OER and the Gutmann Donor Number. Figures S5 and S6 show the correlations between e$^-$/OER and descriptors such as pK_a and the Gibbs activation energy for the nucleophilic substitution reaction, ΔG_{act}, respectively. Figure S7 shows the correlation between the chosen performance metric in this study, e$^-$/O$_2$ during OER and another metric representing total cell rechargeability, (e$^-$/ORR)/(e$^-$/ORR). This material is available free of charge via the Internet at http://pubs.acs.org/.

■ AUTHOR INFORMATION

Corresponding Author
*E-mail: venkvis@cmu.edu.

Notes
The authors declare no competing financial interest.

■ ACKNOWLEDGMENTS

■ REFERENCES

(1) Girishkumar, G.; McCloskey, B.; Luntz, A. C.; Swanson, S.; Wilcke, W. Lithium−Air Battery: Promise and Challenges. *J. Phys. Chem. Lett.* **2010**, *1*, 2193−2203.

(2) Bruce, P. G.; Freunberger, S. A.; Hardwick, L. J.; Tarascon, J.-M. Li−O$_2$ and Li−S Batteries with High Energy Storage. *Nat. Mater.* **2012**, *11*, 19−29.

(3) Lu, Y.-C.; Gallant, B. M.; Kwabi, D. G.; Harding, J. R.; Mitchell, R. R.; Whittingham, M. S.; Shao-Horn, Y. Lithium−Oxygen Batteries: Bridging Mechanistic Understanding and Battery Performance. *Energy Environ. Sci.* **2013**, *6*, 750−768.

(4) Viswanathan, V.; Thygesen, K. S.; Hummelshøj, J. S.; Nørskov, J. K.; Girishkumar, G.; McCloskey, B. D.; Luntz, A. C. Electrical Conductivity in Li$_2$O$_2$ and Its Role in Determining Capacity Limitations in Non-Aqueous Li−O$_2$ Batteries. *J. Chem. Phys.* **2011**, *135*, 214704.

(5) Viswanathan, V.; Nørskov, J. K.; Speidel, A.; Scheffler, R.; Gowda, S.; Luntz, A. C. Li−O$_2$ Kinetic Overpotentials: Tafel Plots from Experiment and First-Principles Theory. *J. Phys. Chem. Lett.* **2013**, *4*, 556−560.

1322

dx.doi.org/10.1021/jz500485r | J. Phys. Chem. Lett. 2014, 5, 1318−1323

(6) Varley, J. B.; Viswanathan, V.; Nørskov, J. K.; Luntz, A. C. Lithium and Oxygen Vacancies and Their Role in Li_2O_2 Charge Transport in $Li-O_2$ Batteries. *Energy Environ. Sci.* **2014**, *7*, 720−727.

(7) Luntz, A. C.; Viswanathan, V.; Voss, J.; Varley, J. B.; Nørskov, J. K.; Scheffler, R.; Speidel, A. Tunneling and Polaron Charge Transport through Li_2O_2 in $Li-O_2$ Batteries. *J. Phys. Chem. Lett.* **2013**, *4*, 3494−3499.

(8) McCloskey, B. D.; Bethune, D. S.; Shelby, R. M.; Mori, T.; Scheffler, R.; Speidel, A.; Sherwood, M.; Luntz, A. C. Limitations in Rechargeability of $Li-O_2$ Batteries and Possible Origins. *J. Phys. Chem. Lett.* **2012**, *3*, 3043−3047.

(9) McCloskey, B. D.; Scheffler, R.; Speidel, A.; Girishkumar, G.; Luntz, A. C. On the Mechanism of Nonaqueous $Li-O_2$ Electrochemistry on C and Its Kinetic Overpotentials: Some Implications for Li−Air Batteries. *J. Phys. Chem. C* **2012**, *116*, 23897−23905.

(10) Laoire, C. O.; Mukerjee, S.; Abraham, K. M.; Plichta, E. J.; Hendrickson, M. A. Elucidating the Mechanism of Oxygen Reduction for Lithium−Air Battery Applications. *J. Phys. Chem. C* **2009**, *113*, 20127−20134.

(11) Laoire, C. O.; Mukerjee, S.; Abraham, K. M.; Plichta, E. J.; Hendrickson, M. A. Influence of Nonaqueous Solvents on the Electrochemistry of Oxygen in the Rechargeable Lithium−Air Battery. *J. Phys. Chem. C* **2010**, *114*, 9178−9186.

(12) Bryantsev, V. S.; Giordani, V.; Walker, W.; Blanco, M.; Zecevic, S.; Sasaki, K.; Uddin, J.; Addison, D.; Chase, G. V. Predicting Solvent Stability in Aprotic Electrolyte Li−Air Batteries: Nucleophilic Substitution by the Superoxide Anion Radical ($O_2^{\cdot-}$). *J. Phys. Chem. A* **2011**, *115*, 12399−12409.

(13) Bryantsev, V. S.; Uddin, J.; Giordani, V.; Walker, W.; Addison, D.; Chase, G. V. The Identification of Stable Solvents for Nonaqueous Rechargeable Li−Air Batteries. *J. Electrochem. Soc.* **2013**, *160*, A160−A171.

(14) Bryantsev, V. S.; Faglioni, F. Predicting Autoxidation Stability of Ether- and Amide-Based Electrolyte Solvents for Li−Air Batteries. *J. Phys. Chem. A* **2012**, *116*, 7128−7138.

(15) Bryantsev, V. S. Predicting the Stability of Aprotic Solvents in Li−Air Batteries: pK_a Calculations of Aliphatic C−H Acids in Dimethyl Sulfoxide. *Chem. Phys. Lett.* **2013**, *558*, 42−47.

(16) Bryantsev, V. S.; Blanco, M. Computational Study of the Mechanisms of Superoxide-Induced Decomposition of Organic Carbonate-Based Electrolytes. *J. Phys. Chem. Lett.* **2011**, *2*, 379−383.

(17) McCloskey, B. D.; Valery, A.; Luntz, A. C.; Gowda, S. R.; Wallraff, G. M.; Garcia, J. M.; Mori, T.; Krupp, L. E. Combining Accurate O_2 and Li_2O_2 Assays to Separate Discharge and Charge Stability Limitations in Nonaqueous $Li-O_2$ Batteries. *J. Phys. Chem. Lett.* **2013**, *4*, 2989−2993.

(18) McCloskey, B. D.; Speidel, A.; Scheffler, R.; Miller, D. C.; Viswanathan, V.; Hummelshøj, J. S.; Nørskov, J. K.; Luntz, A. C. Twin Problems of Interfacial Carbonate Formation in Nonaqueous $Li-O_2$ Batteries. *J. Phys. Chem. Lett.* **2012**, *3*, 997−1001.

(19) Trasatti, S. The Absolute Electrode Potential: An Explanatory Note. *Pure Appl. Chem.* **1986**, *58*, 955−966.

(20) Radin, M. D.; Siegel, D. J. Charge Transport in Lithium Peroxide: Relevance for Rechargeable Metal−Air Batteries. *Energy Environ. Sci.* **2013**, *6*, 2370−2379.

(21) Hummelshøj, J. S.; Blomqvist, J.; Datta, S.; Vegge, T.; Rossmeisl, J.; Thygesen, K. S.; Luntz, A. C.; Jacobsen, K. W.; Nørskov, J. K. Communications: Elementary Oxygen Electrode Reactions in the Aprotic Li−Air Battery. *J. Chem. Phys.* **2010**, *132*, 071101.

(22) Ong, S. P.; Mo, Y.; Ceder, G. Low Hole, Polaron Migration Barrier in Lithium Peroxide. *Phys. Rev. B* **2012**, *85*, 081105.

(23) Geng, W. T.; He, B. L.; Ohno, T. Grain Boundary Induced Conductivity in Li_2O_2. *J. Phys. Chem. C* **2013**, *117*, 25222−25228.

(24) Kang, J.; Jung, Y. S.; Wei, S.-H.; Dillon, A. C. Implications of the Formation of Small Polarons in Li_2O_2 for Li−Air Batteries. *Phys. Rev. B* **2012**, *85*, 035210.

(25) Garcia-Lastra, J. M.; Myrdal, J. S. G.; Christensen, R.; Thygesen, K. S.; Vegge, T. DFT+U Study of Polaronic Conduction in Li_2O_2 and Li_2CO_3: Implications for Li−Air Batteries. *J. Phys. Chem. C* **2013**, *117*, 5568−5577.

(26) Garcia-Lastra, J. M.; Rostgaard, C.; Rubio, A.; Thygesen, K. S. Polarization-Induced Renormalization of Molecular Levels at Metallic and Semiconducting Surfaces. *Phys. Rev. B* **2009**, *80*, 245427.

(27) Radin, M. D.; Rodriguez, J. F.; Tian, F.; Siegel, D. J. Lithium Peroxide Surfaces Are Metallic, While Lithium Oxide Surfaces Are Not. *J. Am. Chem. Soc.* **2012**, *134*, 1093−1103.

(28) Johnson, R. D., III, Ed. NIST Computational Chemistry Comparison and Benchmark Database - NIST Standard Reference Database Number 101. 2013; http://cccbdb.nist.gov/.

(29) Viswanathan, V.; Hansen, H. A. Unifying Solution and Surface Electrochemistry: Limitations and Opportunities in Surface Electrocatalysis. *Top. Catal.* **2014**, *57*, 215−221.

(30) Popov, A. Alkali Metal NMR and Vibrational Spectroscopic Studies on Solvates in Non-Aqueous Solvents. *Pure Appl. Chem.* **1975**, *41*, 275−289.

(31) Aurbach, D.; Weissman, I. In *Nonaqueous Electrochemistry*; Aurbach, D., Ed.; Marcel Dekker: New York, 1999; Chapter 1.

(32) Chickos, J.; Acree Jr., W.; Liebman, J.; Heat of Fusion Data. In *NIST Chemistry WebBook*; NIST Standard Reference Database Number 69; Linstrom, P. J., Mallard, W. G., Eds.; National Institute of Standards and Technology: Gaithersburg, MD, 2014.

(33) Brown, R.; Stein, S. Boiling Point Data. In *NIST Chemistry WebBook*; NIST Standard Reference Database Number 69; Linstrom, P. J., Mallard, W. G., Eds.; National Institute of Standards and Technology: Gaithersburg, MD, 2014.